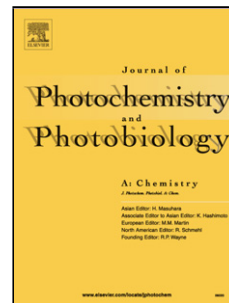# Accepted Manuscript

Title: Solvatochromic properties of a new isocyanonaphthalene based fluorophore

Author: Dávid Rácz Miklós Nagy Attila Mándi Miklós Zsuga Sándor Kéki

Please cite this article as: D. Rácz, M. Nagy, A. Mándi, M. Zsuga, S. Kéki, Solvatochromic properties of a new isocyanonaphthalene based fluorophore, *Journal of Photochemistry and Photobiology A: Chemistry* (2013), http://dx.doi.org/10.1016/j.jphotochem.2013.07.007

Solvatochromic properties of a new isocyanonaphthalene based fluorophore

Dávid Rácz[1], Miklós Nagy[1], Attila Mándi[2], Miklós Zsuga[1], Sándor Kéki[1]*

[1]Department of Applied Chemistry, University of Debrecen, Egyetem tér 1., H-4032 Debrecen, Hungary

[2]Department of Organic Chemistry, University of Debrecen, Egyetem tér 1., H-4032 Debrecen, Hungary

* Corresponding author: keki.sandor@science.unideb.hu, tel: +36 52 512900/22480, fax: +36 52 518662; *H-4032 Debrecen, HUNGARY*

Abstract

The photophysical properties of a new naphthalene based fluorophore, namely the 1-amino-5-isocyanonaphthalene (ICAN) investigated by steady-state and time-resolved fluorescence methods are reported. The molecule showed positive solvatochromic properties, that is a more than $\Delta \bar{v}$ =4800 cm^{-1} red-shift of the emission maximum was observed (from 409 nm in hexane to 513 nm in water). The fluorescence quantum efficiency was found to decrease with increasing solvent polarity, from an excellent Φ_F=0.95 in 1,4-dioxane to Φ_F=0.04 in water. The Kamlet-Taft theory turned out to give the most appropriate description of the solvatochromic properties of the ICAN in various solvents including both protic and non-protic solvents. By carrying out experiments in cyclohexane/tetrahydrofuran binary mixtures of different compositions, evidence was found for the preferential solvation of ICAN. Based on laser light flash photometry measurements the radiative decay rate of ICAN were determined for six different solvents of largely different polarity. The decay rates show only minor solvent dependence and the life-times of the excited states are in the order of 10 ns which are in good agreement with the calculated values. The practical applicability of ICAN was demonstrated by determining the critical micelle concentration of sodium laurylsulfate in water.

Keywords: Fluorescence, solvent-dependence, Kamlet-Taft equation, Stokes-shift, preferential solvation

1

1. Introduction

Since the discovery of fluorescence in the mid-1800s the development and investigation of new fluorophores have always been an exciting field of research. During the last few decades the application of fluorescence spectroscopy has seen a remarkable growth in biological sciences. In conjunction with time resolved fluorescence they are considered to be one of the primary research tools in biochemistry and biophysics [1]. It has long been known that absorption/emission spectra of chemical compounds may be influenced by the surrounding medium and that solvents can bring about a change in the position, intensity, and shape of absorption bands [2]. This phenomenon is generally known as solvatochromism, however, it cannot be limited to solvated particles only, it was also observed in solids, and on various surfaces/interfaces. Solvatochromism is caused by differential solvation of the ground and first excited state of the light-absorbing molecule. Based on its ability to detect the bulk or local polarity, solvatochromism is commonly used in many fields of chemical and biological research in macrosystems (membranes, etc.), where fluorescent probes provide a very sensitive, non-destructive way for the detection of biomolecules and their interactions [3-5]. Besides solvent polarity indicators solvatochromic dyes in general, are useful for creating solutions that absorb light at a specific frequency, as pH sensors and transition metal cation indicators [6-9]. When dealing with solvent effects, polarization, solubility, solute−solvent hydrogen-bonding interactions, and solute aggregation must be taken into consideration. Among many review articles covering this field [2,3,10,11], Marini et al in their recent study gave a description of the phenomenon using quantum chemical approach [12]. However, solvatochromism still remains largely unknown due to the complex coupling of these many different interactions. Besides, the number of practically applicable fluorescent solvatochromic molecules is limited to a few dozen. Naphthalene derivatives, such as 6-lauroyl and 6-propiony1-2-dimethylamino naphthalene, LAURDAN and PRODAN, are among the most common solvatochromic fluorophores [13-15]. The fluorescent naphthalene moiety of these probes possesses a dipole moment due to a partial charge separation between the 2-dimethylamino and the 6-carbonyl residues. This dipole moment increases upon excitation and may cause reorientation of the solvent dipoles. It is assumed, that charge separation can also be accomplished when the acceptor carbonyl is exchanged to an isocyano group. To our best knowledge nobody has prepared naphthalenes bearing amino and isocyano groups at the same time. The isocyano (NC) group is well known of its π-backbonding properties [16,17]. Isocyanides can also function as strong proton acceptor groups in hydrogen bonding through the carbon atom [18], making suitable the molecule not only for

2

the detection of changes in polarity but also for the possible detection of hydrogen donor groups such as OH and NH in the proximity of the molecule. Isocyanides form stable complexes with transition metal ions such as Cu^{2+}, Ag^+ and Au^+ leading to the preparation of possible solvatochromic isocyano complexes [19,20].

Hereby we report the synthesis and detailed steady state and time-dependent fluorescence study of a new solvatochromic fluorophore, namely the 1-amino-5-isocyanonaphthalene.

2. Experimental

2.1. Materials

Acetone, dichloromethane (DCM), hexane, 2-propanol (iPrOH), toluene, (reagent grade, Molar Chemicals, Hungary) were purified by distillation. Acetonitrile (MeCN), tetrahydrofuran (THF), methanol (MeOH), dimethylformamide (DMF), dimethyl sulfoxide (DMSO), pyridine (HPLC grade, VWR, Germany), chloroform, ethyl acetate (EtOAc), ethanol (EtOH) (reagent grade, Molar Chemicals, Hungary), cyclohexane, 1,4-dioxane (reagent grade, Reanal, Hungary), 1,5-diaminonaphthalene, poly(ethylene glycol) (PEG) and poly(propylene glycol) (PPG) (Sigma-Aldrich, Germany) were used without further purification. A pure sample of 1,5-diisocyanonaphthalene was received from Prof. Pál Herczegh at the Department of Pharmaceutical Chemistry, University of Debrecen.

2.1.1. 1-amino-5-isocyanonaphthalene

The synthesis and characterization of the molecule is presented in the *Supporting Information*.

2.2. Methods

The UV-Vis spectra were recorded on a HP 8453 diode array spectrophotometer in a quartz cuvette of 1 cm optical length. 3.00 cm^3 solution was prepared from the sample.

Fluorescence measurements were carried out using a Jasco FP-8200 fluorescence spectrophotometer equipped with a Xe lamp light source. The excitation and emission spectra were recorded at room temperature, using 2.5 nm excitation, 5.0 nm emission bandwith, and 100 nm/min scanning speed. Fluorescence quantum yields were calculated by using quinine-sulfate in 0.1 mol/L sulfuric acid as the reference absolute quantum efficiency ($\Phi_n = 55\%$).

For UV-Vis and fluorescence measurments ICAN was dissolved in the solvents at concentration of 0.2 mg/ml (1.19 mM) and was diluted to 4.00 mg/l ($2.38*10^{-5}$ M) and 0.800 mg/l ($4.76*10^{-6}$ M).

3

Solutions for determining CMC of sodium laurylsulfate was prepared by mixing the aqueous solution of sodium laurylsulfate (0.0164 M) and water in appropriate ratio to have 2.952 ml solution and adding 48 μl of ICAN (0.050 mg/ml, $2.97*10^{-4}$ M) dissolved in DMSO.

Laser flash photolysis experiments have been carried out in an Applied Photophysics LKS.60 nanosecond transient absorption spectrometer, equipped with a Quantel Brilliant Nd:YAG laser along with its second, third and fourth harmonic generator. Fourth harmonic was used, which emits at 266 nm.

2.3. Computational section

The ICAN molecule was optimized at the B3LYP/6-31G(d) *in vacuo*, B3LYP/TZVP *in vacuo* and with PCM solvent model for hexane, MeCN and DMSO, and B97D/TZVP *in vacuo* levels of theory implemented in the Gaussian 09 package [21]. ESP (Merz–Kollman) charges were computed at all levels [22,23]. TD-DFT calculations were performed on the optimized geometries using TZVP basis set and various functionals (B3LYP. BH&HLYP, PBE0). UV spectra were calculated from the oscillator strength values with 2700 cm^{-1} half-height width.

3. Results and Discussion

1-naphthylamine (1-NA) is a well-known fluorophore, whose solvatochromic properties have been discussed in the literature earlier [24,25]. Although 1-NA has high quantum yields, its emission maximum in most solvents falls in the UV region making visible detection very hard. In addition its Stokes shifts are also moderate (~3600-7000 cm^{-1}, hexane-methanol). Our aim was to synthesize a new, effective, naphthalene based fluorophore which contains an amino group (donor) and an isocyano group (acceptor) at the same time. Therefore, we prepared 1-amino-5-isocyanonaphthalene from 1,5-diaminonaphthalene by the reaction with dichlorocarbene as presented in Scheme 1.

Scheme 1.

Fluorescence spectra of the 1-amino-, 1,5-diamino-, 1,5-diisocyano- and 1-amino-5-isocyanonaphthalene were recorded in THF and the resulting spectra are presented in Fig. 1.

Fig. 1.

4

As it is apparent from Fig. 1., the emission maximum of both the 1,5-diamino- and 1,5-diisocyanonaphthalene is found under 400 nm in the UV region. The emission maximum of 1-NA in THF is found at 405 nm, while in the case of ICAN the emission peak is largely shifted to the bathochromic direction and located at 464 nm in the blue region of the visible spectrum. That is, the introduction of an isocyano group at the 5 position of the naphthalene ring resulted in an almost 60 nm red shift of the emission maximum. The excitation peaks of ICAN can also be found at higher wavelengths than those of the three other compounds. The shape of the excitation spectrum of ICAN is similar to that of the 1,5-diaminonaphthalene as both contain two peaks above 300 nm, originating from two vibrational energy levels. At the same time the second excitation band of 1,5-diisocyanonaphthalene is the superposition of 5 vibrational energy levels with narrower peaks indicating a more rigid structure. In addition, ICAN has a relatively large Stokes shift of 7564 cm^{-1} which was found to be further increasing in polar solvents such as methanol, that is, the color of the emitted light turned from blue in THF to green in MeOH when irradiated with $\lambda= 365$ nm UV light. The explanation for the large Stokes shift and the solvatochromic behavior of ICAN can be charge transfer between the amino and isocyano groups of the molecule. To test this assumption the detailed UV/VIS and fluorescence study of ICAN followed.

3.1.   UV/VIS and steady-state fluorescence properties

The UV/VIS and excitation spectra of 1-amino-5-isocyanonaphthalene dissolved in a variety of solvents show two main absorption bands located at near 260, 340 and 360 nm. (The absorbance spectra match the excitation spectra.) The characteristics of the excitation spectra of 1-amino-5-isocyanonaphthalene are compiled in Table 1. and the excitation spectra obtained in some selected solvents are shown in Fig. 2. a.

Table 1.

Fig. 2.

As seen from the data of Table 1. and Fig. 2a. all absorption bands show moderate red shift in going from non-polar to polar solvents. The same effect can be observed on the computed spectra, too. See Figs. S6-S8. in the SI. The positions of band λ_1 assigned to the S_o-S_2 transition varies between 251-269 nm, while those of bands λ_2 and λ_3, change in the range of 336-347 and 350-373 nm. The shapes of bands λ_2 and λ_3 change with the solvent polarity (Fig.

5

2a.). The latter two bands are assigned to the S_o-S_1 transition coupled with vibrational modes of the same electronic transition (S_o-S_1). The differences between bands λ_2 and λ_3 are close to 1500 cm^{-1} on the average which approximately corresponds to the value of C=C vibronic elongation. All 3 levels of theory applied for computing the UV spectra on the optimized conformer resulting from all optimizations yielded only one low-energy transition, which also indicates that splitting of this transition has to be occurred that further verifies the assumption of vibrational modes. Interestingly, the molar absorption coefficient (ε) determined at band λ_2 shows no considerable change upon the effect of solvent polarity, the value of ε is approximately 6000 M^{-1}cm^{-1}. Furthermore, it is also apparent from Table 1. that considerable red-shift can be observed in the fluorescence emission spectra of ICAN with solvent polarity. It can be recognized that in hexane the emission spectrum is a "mirror" of the excitation spectrum falling in the range of 340-360 nm. However, with increasing solvent polarity the fine emission band structure (shoulder at longer wavelength) disappears, yielding single emission bands. It is also important to emphasize that the shape and the wavelength at the maximum emission intensity are independent of the excitation wavelength, i.e., similar emission spectra were obtained using shorter excitation wavelengths (in the range of 250-260 nm). The characteristics of fluorescence emission of ICAN in various solvents are summarized in Table 2. The solvent-dependent fluorescence properties of ICAN are demonstrated in Fig. 3.

Table 2.

Fig. 3.

As seen in Fig. 3. and Table 2. the 1-amino-5-isocyanonaphthalene dissolved in a variety of solvents shows strong fluorescence emission with wavelengths ranging from λ=409 nm (blue) up to λ=513 nm (green). It can be surmised from Table 2. that relatively high quantum yields were obtained both in polar and non-polar solvents except for the case of water. In water, only very low quantum yield was obtained (Φ_F=0.04) and it can be inferred that in water transition from state S_1 to S_o takes place mainly by non-radiative processes. Furthermore, according to the data of Table 2., the emission band maxima vary significantly with the solvent polarity. (The excitation wavelengths were chosen at the absorbance maxima.) As it was mentioned earlier the excitation spectra match the absorbance spectra and the emission spectra are independent of the excitation wavelengths indicating that electronic transition occurs from

6

each excited state to the same lowest ground state. At the simplest level, the shifts to higher fluorescence emission maxima and/or the Stokes shifts ($\Delta \bar{v}$), i.e., the difference between the wavenumbers at absorption ($\bar{v}_a$) and emission maxima ($\bar{v}_e$) can be interpreted in terms of increasing solvent polarity (see Figure S4 in the supporting information).

Indeed, the Stokes shifts and the fluorescence emission maxima are shifted to higher wavenumbers as the solvent dielectric constant increases. To rationalize the effect of the solvent on the fluorescence emission spectra the Lippert-Mataga equation is applied (eq. 1)

$$\Delta \bar{v} = \frac{2(\mu_e - \mu_g)^2}{4\pi\varepsilon_o hca^3} \Delta f + \text{const} \tag{1}$$

where $\Delta \bar{v}$ (in cm^{-1}) is the Stokes shift, μ_e and μ_g are the dipole moments of the excited and the ground states, respectively. h, c and ε_o are the Planck's constant, speed of the light in vacuum and the permittivity of the vacuum, respectively. a is the radius of a spherical cavity in which the fluorophore molecule resides. Δf is the orientation polarizability that can be expressed as: $\Delta f = \frac{\varepsilon - 1}{2\varepsilon - 1} - \frac{n^2}{2n^2 - 1}$, where ε and n are the dielectric constant and the refractive index of the solvent, respectively.

From Eq. 1 the well-known Lippert-Mataga plot can be constructed. However, there are some restrictions for the use of eq. 1. (i) It is assumed that the dipole moments of the different states (excited and ground) of the fluorophore and the solvent are not altered by the interactions. (ii) Emissions take place from the relaxed excited state of the fluorophore. (iii) There are no specific interactions between the solvent molecules and either state of the fluorophores. This latter can be expected when using protic solvents e.g. solvent with OH group or solvents capable of forming hydrogen bond with the fluorophore molecules. Using the Lippert-Mataga Δf values of solvents listed in Table 2. except for those of protic the Lippert-Mataga plot is constructed that is shown in Fig. 4.

Fig. 4.

As it can be seen in Fig. 4. a linear trend for the $\Delta \bar{v}$ versus Δf data with an acceptable correlation (r=0.87) can be observed. From the slope of the line presented in Fig. 4. the

7

transient dipole moment, i.e., the value of μ_e-μ_g can be derived by assuming a reasonable cavity radius of ~0.4 nm (the radius of the cavity was estimated based using $a_o = [3M/(4\pi N_A \rho)]^{1/3}$ where M is the molecular weight, N_A is the Avogadro`s constant and ρ is the density estimated to be ~1 g/cm^3). Based on this estimate a value of ~7 D was obtained for $\Delta\mu$ which value is very similar to that of PRODAN, a well-known fluorophore [26,27]. Quantum chemical calculations were carried out for ICAN dissolved in MeCN and DMSO (see Tables S2 and S3). The dipole moment differences between the ground and the excited states obtained: $\Delta\mu$=6.71 D in MeCN and $\Delta\mu$=6.73 D in DMSO are in good agreement with the estimated one of ~7 D. By considering the value of $\Delta\mu$ and the distance between the separated charges (~0.8 nm) it can also be estimated that shift of the charge from the amine nitrogen toward the isocyano group is not complete, and a ~$\pm$0.2 partial charge separation can be estimated on the donor (amine) and the acceptor (isocyano) groups in the excited state with respect to the ground state.

As it was emphasized earlier the Lippert-Mataga theory is not capable of considering specific interaction between the solvent and the fluorophore. The Δf parameter takes into account the properties associated with the permanent dipoles (ϵ) and the polarizability (n). On the other hand, although the Lippert-Mataga plot shows a clear linear trend between $\Delta\bar{\nu}$ and Δf the large scattering in the data may indicate that the orientation not only the orientation polarizibility (Δf) is the factor that affects the Stokes shift. Therefore, for the more complete description of the solvatochromic properties of the ICAN in various solvents including both protic and non-protic solvents the Kamlet-Taft theory seems to be promising since it considers not only the polarity/polarizability but also the acidity and the basicity of the solvents [28]. According to the Kamlet-Taft theory the change of the properties (Y) including e.g. the shift of the absorption ($\bar{\nu}_{abs,max}$) or emission band ($\bar{\nu}_{em,max}$) maxima or Stokes shifts ($\Delta\bar{\nu}$) are a linear combination of three solvent-dependent parameters as shown in eq. 2.

$$Y = Y_o + a\alpha + b\beta + c\pi^*$$ (2)

where Y_o is the property of substance in interest in the absence of solvent e.g. in the gas-phase, α, β and π^* are the solvent parameters that characterize the acidity, the basicity and polarity/polarizability of the solvent, respectively. a, b and c are the corresponding coefficients. Applying eq. 2. for the emission wavenumber at the maximum ($\bar{\nu}_{em,max}$) and the

8

Stokes shifts ($\Delta\bar{\nu}$) as well as using the corresponding α, β and π^* values of the solvents (the α, β and π^* values of the solvents used in this study are given in the Supplementary Information in Table S1. [29,30]) the Kamlet-Taft coefficients for $\bar{\nu}_{em,max}$ and $\Delta\bar{\nu}$ can be obtained by multilinear regression analysis. According to these regression analysis for $\bar{\nu}_{em,max}$ and $\Delta\bar{\nu}$ the following relationships can be established:

$$\bar{\nu}_{em,max} (cm^{-1}) = (23890 \pm 220) - (767 \pm 234)\alpha - (2256 \pm 373)\beta - (2360 \pm 350)\pi^* \qquad (3)$$

$$\Delta\bar{\nu} (cm^{-1}) = (5640 \pm 230) + (1254 \pm 242)\alpha + (1390 \pm 386)\beta + (2280 \pm 360)\pi^* \qquad (4)$$

It should be noted that no cross-correlation between the fitted parameters were found. For the sake of better visualization of the experimental and the fitted data, the measured values of $\bar{\nu}_{em,max}$ and $\Delta\bar{\nu}$ are plotted in Fig. 5. as a function of their corresponding values calculated by eq. 3 and eq. 4., respectively.

Fig. 5.

As seen in Fig. 5a. and Fig. 5b. the measured values for $\bar{\nu}_{em,max}$ and $\Delta\bar{\nu}$ are correlated well with those of the calculated by eqs. 3-4. and the slopes of the fitted lines with a regression coefficients of r=0.97 for both cases are very close to unity. As a result of these calculations, it is now evident that the Kamlet-Taft theory is capable of describing the solvatochromic behavior of ICAN in a wide variety of solvents (including non-protic and protic, too). Furthermore, the Kamlet-Taft theory was also applied to the description of the shift excitation/absorption band λ_2. It was found that the solvent acidity parameter (α) does not affect the absorption maxima. In Fig. 6. the excitation/absorption spectra of ICAN dissolved in DMF, pyridine and PEG are shown in the range of 250-450 nm.

Fig. 6.

As seen in Fig. 6. the three spectra are very similar to each other considering both their maxima and shapes. This large similarity can easily be rationalized by taking into account the Kamlet-Taft parameters of these solvents. The Kamlet-Taft parameters of DMF (α=0, β=0.68 and π^*=0.88) are very similar to those of pyridine (α=0, β=0.64 and π^*=0.84). On the

9

contrary, although the Kamlet-Taft β and π^* of PEG are very similar to those of DMF and pyridine, the α value of PEG (0.31) differs significantly yet the PEG excitation spectrum is very similar to those of DMF and pyridine, i.e., α has no considerable influence on the excitation/absorption spectra in the range of 250-450 nm.

After the investigation of the optical properties of ICAN in pure solvents, experiments were performed with binary mixtures of solvents of different compositions, in order to get deeper insight into the possible preferential solvation of ICAN. For this purpose, solvents cyclohexane and tetrahydrofuran (THF) were selected and emission maxima of ICAN as a function of the solvent compositions were studied. Fig. 7. shows the variation of the emission maximum of ICAN in solvent mixtures with different compositions expressed by the molar fractions of THF.

Fig. 7.

If there is no preferential solvation, which represents an ideal situation, then the observed emission maximum ($\bar{v}_{em,max}$) should be a linear combinations of the emission maxima obtained separately in the pure solvents as given by eq. 5.

$$\bar{v}_{em,max}(ideal) = \bar{v}_{em,max1}(1 - X_2) + \bar{v}_{em,max2}X_2 \tag{5}$$

where $\bar{v}_{em,max1}$ and $\bar{v}_{em,max2}$ are the emission maxima observed in solvent 1 and solvent 2, and X_2 is the molar fraction of solvent 2 in the mixture (Usually the more polar solvent is denoted by solvent 2, in our case it is the THF).

As it is clear from Fig. 7a. the measured values of $\bar{v}_{em,max}$ deviate considerably from the ideal case which indicates that preferential solvation for ICAN exists in the cyclohexane-THF mixture. Preferential solvation can cause solvent compositions that are different in the local environment of the fluorophore and in the bulk. Since the fluorescence emissions of fluorophores are sensitive to their local environment, the local composition can be calculated using eq. 6

$$X_2{}^L = \frac{\bar{v}_{em,max} - \bar{v}_{em,max1}}{\bar{v}_{em,max2} - \bar{v}_{em,max1}} \tag{6}$$

10

where X_2 and X_2^L are the molar fractions of the solvent 2 in the bulk and in the local environment of the fluorophore, respectively.

As it is apparent from Fig. 7b. the local molar fraction of THF is much higher than in the bulk indicating the preferential solvation of THF over cyclohexane. For the description of the preferential solvation effect presented in Fig. 7. the two-step solvent-exchange model is applied [31]. Although this model has been particularly applied for solvent mixtures containing hydrogen bond acceptor (solvents with higher β) and hydrogen bond donor (solvents with higher α) solvents [32,33] the application of this model to the cyclohexane-THF mixture seems to be also promising (due to the expected non-polar interaction between the hexane and THF). The preferential solvation model by the two-step solvent exchange can be formulated by eq. 7.

$$\overline{\nu}_{em,max} = \frac{\overline{\nu}_{em,max1}(1-X_2)^2 + \overline{\nu}_{em,max2}f_{2/1}X_2^2 + \overline{\nu}_{em,max12}f_{12/1}(1-X_2)X_2}{(1-X_2)^2 + f_{2/1}X_2^2 + f_{12/1}(1-X_2)X_2} \qquad (7)$$

where $f_{2/1}$, and $f_{12/1}$ are the extent of solvation of the fluorophore by solvent 2, and solvent 1 and 2 relatively to solvent 1, respectively. $\overline{\nu}_{em,max12}$ is the emission maximum when the solvation shell contains solvent 1 and solvent 2 molecules evenly.

Eq. 7 was fitted to the experimental $\overline{\nu}_{em,max}$ *versus* X_{THF} data and the values of $f_{2/1}$, $f_{12/1}$ and $\overline{\nu}_{em,max12}$ were determined. As seen in Fig. 7a. the curve calculated by eq. 7 fits well to the experimental one (dashed line). Furthermore, based on eq. 6 and eq. 7 the local molar fraction of THF can also be calculated (Fig. 7b. dashed line). The experiments were also carried out using 1-naphthylamine (1-NA) to test the role of the amino group in the solvent exchange process. The results are presented in Figure S5 in the SI. 1-NA also shows preferential solvation, what is more in a more expressed manner compared to ICAN. At 6.5 % (n/n) THF content in the bulk solution, more than 60 % (n/n) THF can be found in the local environment of 1-NA, while this number is only 53 % (n/n) in the case of ICAN. Considering the large β-parameter of THF and the similar solvation behavior of 1-NA and ICAN we may conclude that the driving force of this preferential solvation is the strong H-bonding interaction between the amino group and the THF oxygen.

11

3.2.   *Time-resolved fluorescence properties*

Time-resolved fluorescence properties of ICAN were studied using laser light flash photometry as outlined in the Experimental. For the flash photolysis experiment six solvents which differed greatly in their polarity were selected. Using a laser with an excitation wavelength of 266 nm brings the system from the state S_o to S_2. However, transition from state S_2 to S_1 occurs much faster (by non-radiative process) than the time required for S_1-S_o transition. As discussed earlier the excitation wavelength has no influence on the resulting fluorescence spectra. Fig. 8. shows the fluorescence spectra of ICAN in acetonitrile recorded at different times. For the sake of comparison the steady-state fluorescence spectrum is also added.

Fig. 8.

As can be seen in Fig. 8. no change of the shape of the fluorescence spectra can be observed and the transient fluorescence spectra match closely that obtained by steady-state measurement.

The radiative decay rate (k_F) can be calculated from the absorption and emission spectra using the Strickler-Berg equation (eq. 8.) [34]

$$k_F(s^{-1}) = 2.88 \times 10^{-9} n^2 \frac{\int F(\overline{v}) d\overline{v}}{\int F(\overline{v}) \overline{v}^{-3} d\overline{v}} \int \frac{\varepsilon(\overline{v})}{\overline{v}} d\overline{v} \tag{8}$$

where n is the refractive index of the solvent, $\varepsilon(\overline{v})$ is the molar absorption coefficient and $F(\overline{v})$ is the fluorescence intensity at wave number $\overline{v}$.

The radiative decay rate (k_F) can be given from the decay rate (k) using eq. 9.

$$k_F = \Phi_F k \tag{9}$$

where Φ_F is the quantum yield.

The decay rate (k), the measured and the calculated radiative decay rate by eq. 9. for six different solvents are summarized in Table 3.

Table 3.

12

As seen from the data of Table 3. the decay rates vary only in minor extent with the solvent polarity. The life-times (τ) of the excited states in the solvents listed are in the order of 10 ns (based on $\tau = 1/k$). The shortest and the longest life-times were observed in hexane (6.4 ns) and dimethyl sulfoxide (16.3 ns), respectively. It is also evident that the calculated radiative decay rates agree well with those of the measured ones. The largest deviation can be observed in the case of dimethyl sulfoxide.

3.3. *Practical application of ICAN*

Solvatochromic fluorophores such as PRODAN are used to test the polarity conditions inside or on the surface region of nanodisperse systems (bilayers, membranes, micelles). Based on its nonpolar character, ICAN is expected to interact with, or incorporate in the core of self-assembled nanostructures with hydrophobic core. Long-chain hydrocarbon surfactants such as sodium laurylsulfate can be considered as good model compounds to test the interactions mentioned above. Therefore, the changes of the fluorescence intensity and emission maxima of ICAN dissolved in water were studied in the presence of sodium laurylsulfate (SLS) (Fig.9).

Fig. 9.

As it can be inferred from Fig. 9. the emission intensity increases and the emission maxima is shifted to the blue upon increasing the concentration of SLS. At a certain value of SLS concentration both the emission intensity and maximum reveal abrupt changes. The sharp increase in the emission intensity and decrease in the emission maximum occur at the critical micelle concentration (cmc) as depicted in Fig. 9. These observations are in line with the solvatochromic properties of ICAN: at above the cmc the ICAN molecules are embedded in the non-polar core of the micelles formed. The non-polar environment causes a blue shift for the fluorescence emission of ICAN on one hand, and an increase in the quantum yield (note that the quantum yield in water, see Table 2.) on the other. The cmc value of SLS based on Fig. 9.a and Fig.9.b were determined to be 6.2×10^{-3} mol/L. The cmc was determined independently by conductometry and was found to be 7.3×10^{-3} mol/L. Both values are in an acceptable agreement with the reported value (8×10^{-3} mol/L).

13

4. Conclusions

We prepared a new fluorophore by the reaction of 1,5-diaminonaphtahalene with dichlorocarbene in basic chloroform solution. The resulting 1-amino-5-isocyanonaphtahalene showed strong positive solvatochromic effects. Unlike in the case of the starting 1,5-diamino- and the subsequent 1,5-diisocyanonaphthalene, the emission maxima fell in almost every case in the visible region of the spectrum. The lowest value of 409 nm belonged to the hexane solution, while the highest at 513 nm to the most polar solvent applied, which was water.

The fluorescence quantum efficiency varied between Φ_F=0.95 in 1,4-dioxane and Φ_F=0.04 in water, and was found to decrease with increasing solvent polarity. The shape of the absorption spectra in different media was calculated using time-dependent density function quantum chemical model. The calculated and measured spectra are in good correlation. The Lippert-Mataga plot was applied to describe the solvent polarity effect on the emission spectra; however the Kamlet-Taft equation turned out to give the best results. Samples dissolved in DMF, pyridine and PEG resulted almost the same excitation spectra in the range of 250-450 nm indicating, that the shape of the excitation spectrum can be independent of the acidity parameter of the solvent. The phenomenon of preferential solvation was detected in cyclohexane/THF solutions of ICAN. The radiative decay rates of the excited state were determined by laser light flash photolysis experiments. The shortest and the longest life-times were observed in hexane (6.4 ns) and dimethyl sulfoxide (16.3 ns), respectively and were in the order of 10 ns for most of the solvents studied. Due to its molecular character ICAN prefers nonpolar environments. Based on this property it was demonstrated that ICAN can be applied for the cmc determination of surfactants such as sodium laurylsulfate (SLS) with long nonpolar chain. Above cmc ICAN is located in the nonpolar core of the micelles resulting in a significant blue-shift in emission and increased quantum efficiency.

14

15

References

1. J. R. Lakowicz, *Principles of Fluorescence Spectroscopy*; Springer: New York, 2006.

2. C. Reichardt, Solvatochromic Dyes as Solvent Polarity Indicators. *Chem. Rev.* 94 (1994) 2319-2358.

3. R. M. Epand and R. Kraayenhof, Fluorescent probes used to monitor membrane interfacial polarity. *Chem. Phys. Lipids*, 101, **(**1999) 57–64.

4. H. Bouvrais, T. Pott, L. A. Bagatolli, J. H. Ipsen and P. Méléard, Impact of membrane-anchored fluorescent probes on the mechanical properties of lipid bilayers. *Biochim. Biophys. Acta* 1798 (2010) 1333–1337.

5. S. S. Bag, R. Kundu, K. Matsumoto, Y. Saito and I. Saito, Singly and doubly labeled base-discriminating fluorescent oligonucleotide probes containing oxo-pyrene chromophore. *Bioorg. Med. Chem. Lett.* 20, (2010) 3227–3230.

6. V. D. Suryawanshi, A. H. Gore, L. S. Walekar, P. V. Anbhule, S. R. Patil and G. B. Kolekar, Solvatochromic fluorescence behavior of 2-amino-6-hydroxy-4-(3,4-dimethoxyphenyl)-pyrimidine-5-carbonitrile: A sensitive fluorescent probe for detection of pH and water composition in binary aqueous solutions. *J. Mol. Liq.* (2013), DOI: 10.1016/j.molliq.2013.03.018.

7. N. Kaur and S. Kumar, Colorimetric metal ion sensors. *Tetrahedron* 67 (2011) 9233-9264.

8. M. Baruah, W. Qin, C. Flors, J. Hofkens, R. A. L. Vallee, D. Beljonne, M. Auweraer, W. M. Borggraeve and N. Boens, Solvent and pH dependent fluorescent properties of a dimethylaminostyryl borondipyrromethene dye in solution. *J. Phys. Chem. A* 110 (2006) 5998-6009.

9. E. Hao, T. Meng, M. Zhang, W. Pang, Y. Zhou and L. Jiao, Solvent Dependent Fluorescent Properties of a 1,2,3-Triazole Linked 8-Hydroxyquinoline Chemosensor: Tunable Detection from Zinc(II) to Iron(III) in the CH3CN/H2O System. *J. Phys. Chem. A* 115 (2011) 8234–8241.

10. M. A. Rauf and S. Hisaindee, Studies on solvatochromic behavior of dyes using spectral techniques. *J. Mol. Struct.* 1042 (2013) 45–56.

11. G. S. Loving, M. Sainlos and B. Imperiali, Monitoring protein interactions and dynamics with solvatochromic fluorophores. *Trends Biotechnol.* 28 (2010) 73-83.

16

12. A. Marini, A. Muñoz-Losa, A. Biancardi and B. Mennucci, What is Solvatochromism? *J. Phys. Chem. B* 114 (2010) 17128-17135.

13. T. Parasassi, E. K. Krasnowska, L. Bagatolli and E. Gratton, Laurdan and Prodan as polarity sensitive fluorescence membrane probes. *J. Fluoresc.* 8 (1998) 365-373.

14. S. Hofstetter, C. Denter, R. Winter, L. M. McMullen and M. G. Ganzle, Use of the fluorescent probe LAURDAN to label and measure inner membrane fluidity of endospores of Clostridium spp. *J. Microbiol. Methods* 91 (2012) 93–100.

15. R. Fukuda, R. Chidthong, R. Cammi and M. Ehara, Optical absorption and fluorescence of PRODAN in solution: Quantum chemical study based on the symmetry-adapted cluster-configuration interaction method. *Chem. Phys. Lett.* 552 (2012) 53-57.

16. C. T. Eagle, D. G. Farrar and C. U. Pfaff, J. A. Davies, C. Kluwe, L. Miller, Pi-Back-Bonding in Bis(isonitrile) Complexes of Rhodium(II) Acetate: Structural Analogs for Rhodium Carbenoids. *Organometallics* 17 (1998) 4523–4526.

17. Z. D. Brown, P. Vasko, J. C. Fettinger, H. M. Tuononen and P. P. Power, A Main Group Isonitrile Complex Possessing a (n   pi*) Back-bonding Interaction and Its Conversion to a Hydride/Cyanide Product via C-H Bond Activation under Mild Conditions. *J. Am. Chem. Soc.* 134, (2012) 4045–4048.

18. A. Allerhand and P. R. Schleyer, Nitriles and Isonitriles as Proton Acceptors in Hydrogen Bonding: Correlation of Δv_{OH} with Acceptor Structure. *J. Am. Chem. Soc.* 85 (1963) 866–870.

19. E. Singleton and H. E. Oosthuizen, Metal-isocyanide complexes. *Adv. Organomet. Chem.* 22, (1983) 209-310.

20. M. V. Barybin, J. J. Meyers Jr, and B. M. Neal *Isocyanide Chemistry*; Wiley-VCH: Weinheim, 2012.

21. M. J. Frisch, G. W. Trucks, H. B. Schlegel, G. E. Scuseria, M. A. Robb, J. R. Cheeseman, G. Scalmani, V. Barone, B. Mennucci, G. A. Petersson, H. Nakatsuji, M. Caricato, X. Li, H. P. Hratchian, A. F. Izmaylov, J. Bloino, G. Zheng, J. L. Sonnenberg, M. Hada, M. Ehara, K. Toyota, R. Fukuda, J. Hasegawa, M. Ishida, T. Nakajima, Y. Honda, O. Kitao, H. Nakai, T. Vreven, J. A. Montgomery, Jr., J. E. Peralta, F. Ogliaro, M. Bearpark, J. J. Heyd, E. Brothers, K. N. Kudin, V. N. Staroverov, T. Keith, R. Kobayashi, J. Normand, K. Raghavachari, A. Rendell, J. C. Burant, S. S. Iyengar, J. Tomasi, M. Cossi, N. Rega, J.

17

M. Millam, M. Klene, J. E. Knox, J. B. Cross, V. Bakken, C. Adamo, J. Jaramillo, R. Gomperts, R. E. Stratmann, O. Yazyev, A. J. Austin, R. Cammi, C. Pomelli, J. W. Ochterski, R. L. Martin, K. Morokuma, V. G. Zakrzewski, G. A. Voth, P. Salvador, J. J. Dannenberg, S. Dapprich, A. D. Daniels, O. Farkas, J. B. Foresman, J. V. Ortiz, J. Cioslowski, D. J. Fox, Gaussian 09; Gaussian, Inc.: Wallingford, CT, 2009.

22. U. C. Singh and P. A. Kollman, An approach to computing electrostatic charges for molecules. *J. Comput. Chem.* 5 (1984) 129-145.

23. B. H. Besler, K. M. Merz Jr. and P. A. Kollman, Atomic charges derived from semiempirical methods. *J. Comput. Chem.* 11 (1990) 431-439.

24. J. Dresner, S. H. Modiano and E. C. Lim, Intramolecular photoassociation and photoinduced charge transfer in bridged diaryl compounds. 2. Charge transfer interactions in the lowest excited singlet state of dinaphthylamines. *J. Phys. Chem.* 96 (1992) 4310–4321

25. S. Jiang and D. H. Levy, van der Waals Complex and Solvatochromism Studies of Substituted Benzenes and Naphthalenes, *J. Phys. Chem. A* 107 (2003) 6785–6791

26. O. A. Kucherak, P. Didier, Y. Mély and A. S. Klymchenko, Fluorene analogues of Prodan with superior fluorescence brightness and solvatochromism. *J. Phys. Chem. Lett.* 1 (2010) 616-620.

27. A. Samanta and R.W. Fessenden, Excited state dipole moment of PRODAN as determined from transient dielectric loss measurements. *J. Phys. Chem. A* 104 (2000) 8972-8975.

28. M. J. Kamlet, J. L. M. Abboud, M. H. Abraham and R. W. Taft, Linear solvation energy relationships. 23. A comprehensive collection of the solvatochromic parameters, .pi.*, .alpha., and .beta., and some methods for simplifying the generalized solvatochromic equation. *J. Org. Chem.* 48 (1983) 2877–2887.

29. C. Reichardt and T. Welton *Solvents and Solvent Effects in Organic Chemistry*; Fourth Edition, Wiley-VCH:Weinheim, 2010. p. 313 (table 7.4.)

30. P. G. Jessop, D. A. Jessop, D. Fu and L. Phan, Solvatochromic parameters for solvents of interest in green chemistry. *Green Chem.* 14 (2012) 1245-1259.

31. T. Bevilaqua, T. F. Gonçalves, C. G. Venturini and V. G. Machado, Solute-solvent and solvent-solvent interactions in the preferential solvation of 4-[4-(dimethylamino)styryl]-1-

18

methylpyridinium iodide in 24 binary solvent mixtures. *Spectrochimica Acta Part A*. 65 (2006) 535-542.

32. R. D. Skwierczynski and K. A. Connors, Solvent effects on chemical processes. Part 7. Quantitative description of the composition dependence of the solvent polarity measure ET(30) in binary aqueous-organic solvent mixtures. *J. Chem. Soc., Perkin Trans.* 2 (1994) 467-472.

33. M. A. R. Silva, D. C. Silva, V. G. Machado, E. Longhinotti and V. L. A. Frescura, Preferential Solvation of a Hydrophobic Probe in Binary Mixtures Comprised of a Nonprotic and a Hydroxylic Solvent: A View of Solute−Solvent and Solvent−Solvent Interactions. *J. Phys. Chem. A* 106 (2002) 8820–8826.

34. S. J. Strickler and Robert A. Berg, Relationship between Absorption Intensity and Fluorescence Lifetime of Molecules. *J. Chem. Phys*. 37 (1962) 814-822.

19

Table 1. Excitation maxima of 1-amino-5-isocyanonaphthalene (ICAN) dissolved in different solvents.

No	Solvent*	λ_1 (nm)	λ_2 (nm)	λ_3 (nm)
1	Hexane	252	338	350
2	Toluene	n/a	341	354
3	1,4-Dioxane	259	343	360
4	Tetrahydrofuran (THF)	261	344	365
5	Ethylacetate	260	342	360
6	Dichloromethane	255	340	356
7	Chloroform	254	340	358
8	Poly(propylene glycol) (PPG, M_n=1000 g/mol)	251	345	365
9	Acetone	n/a	345	364
10	Pyridine	n/a	347	368
11	Dimethylformamide(DMF)	269	346	369
12	Acetonitrile	257	342	361
13	Poly(ethylene glycol) (PEG, M_n=400 g/mol)	265	345	367
14	Dimethyl sulfoxide (DMSO)	268	347	372
15	2-Propanol	256	343	361
16	Methanol	256	342	365
17	Water	255	336	-

* Solvents are listed in an increasing order of Stokes shifts

20

Table 2. The wavelengths of excitation (λ_{ex}), fluorescence emission maxima ($\lambda_{em,max}$), Stokes shifts and the quantum yield (ϕ_F) of 1-amino-5-isocyanonaphthalene (ICAN) in various solvents. The Stokes shift is defined as $\Delta\bar{\nu} = \bar{\nu}_{abs,max} - \bar{\nu}_{em,max}$, where $\bar{\nu}_{abs,max}$ and $\bar{\nu}_{em,max}$ are the wavenumbers of absorption (excitation) and emission maxima, respectively.

No	Solvent*	λ_{ex} (nm)	$\lambda_{em,max}$ (nm)	Stokes shift ($\Delta\bar{\nu}$, cm^{-1})	Φ_F
1	Hexane	338	409	5136	0.55
2	Toluene	341	433	6231	0.66
3	1,4-Dioxane	343	458	7320	0.95
4	Tetrahydrofuran (THF)	344	465	7564	0.66
5	Ethylacetate	342	464	7688	0.45
6	Dichloromethane	340	461	7720	0.88
7	Chloroform	340	465	7906	0.63
8	Poly(propylene glycol) (PPG, M_n=1000 g/mol)	345	478	8065	-
9	Acetone	345	479	8109	0.50
10	Pyridine	347	490	8410	0.28
11	Dimethylformamide(DMF)	346	491	8535	0.48
12	Acetonitrile	342	483	8536	0.38
13	Poly(ethylene glycol) (PEG, M_n=400 g/mol)	345	491	8619	-
14	Dimethyl sulfoxide (DMSO)	347	497	8698	0.74
15	2-Propanol	343	494	8912	0.40
16	Methanol	342	494	8997	0.54
17	Water	336	513	10269	0.04

* Solvents are listed in an increasing order of Stokes shifts. The error in the measurements of Φ_F values were within $\pm 10\%$.

21

Table 3. The decay rate (k), the measured ($k_{F,meas}$) and the calculated radiative decay rate ($k_{F,calc}$) obtained for 1-amino-5-isocyanonaphthalene (ICAN) in hexane, tetrahydrofuran, dichloromethane, acetonitrile, methanol and dimethyl sulfoxide (DMSO). The radiative decay rates ($k_{F,calc}$) were calculated using the Strickler-Berg equation (eq. 9.)

Solvent	k (s^{-1})	$k_{F,meas}$ (s^{-1})	$k_{F,calc}$ (s^{-1})
Hexane	1.5×10^8	8.4×10^7	8.1×10^7
Tetrahydrofuran	9.3×10^7	6.2×10^7	7.4×10^7
Dichloromethane	9.8×10^7	8.6×10^7	7.4×10^7
Acetonitrile	1.2×10^8	4.4×10^7	6.0×10^7
Methanol	9.7×10^7	5.2×10^7	4.7×10^7
Dimethyl sulfoxide	6.2×10^7	4.6×10^7	7.1×10^7

* The error in the measurements of k values were within $\pm 10\%$. The Φ_F values listed in Table 1 were used for the calculation of k_F from k.

22

Figure Captions

Scheme 1.
The synthesis of 1-amino-5-isocyanonaphthalene

Figure 1.
The excitation (**a**) and emission (**b**) spectra of 1,5-diisocyanonaphthalene (**DIN**), 1,5-diaminonaphthalene (**DAN**), 1-amino-5-isocyanonaphthalene (**ICAN**) and 1-napthylamine (**1-NA**).

Figure. 2.
Excitation (**a**) and emission spectra (**b**) of 1-amino-5-isocyanonaphthalene (ICAN) in hexane (Hex), tetrahydrofuran (THF), dichloromethane (DCM), 2-propanol (iPrOH) and dimethyl sulfoxide (DMSO).

Figure 3.
Demonstration of the fluorescence properties of 1-amino-5-isocyanonaphthalene (ICAN) in different solvents illuminated by light of λ=365 nm. Solvents from left (blue) to the right (green) are: hexane, toluene, 1,4-dioxane, dichloromethane, ethylacetate, tetrahydrofuran (THF), chloroform, acetone, acetonitrile, pyridine, dimethylformamide (DMF), 2-propanol, methanol, dimethyl sulfoxide (DMSO)

Figure 4.
Change of the Stokes shifts ($\overline{\Delta\nu}$) of 1-amino-5-isocyanonaphthalene (ICAN) as a function of Δf (Lippert-Mataga plot). The numbers at the symbol correspond to the solvents listed in Table 1.

Figure 5.
Plots of the measured and calculated emission maxima (**a**), Stokes shift (**b**) and excitation maxima (**c**) for the 1-amino-5-isocyanonaphthalene (ICAN) obtained by the Kamlet-Taft equation.

Figure 6.
Normalized excitation spectra of 1-amino-5-isocyanonaphthalene (ICAN) obtained in dimethlyformamide (DMF), pyridine and poly(ethylene glycol) (PEG).

Figure 7.
(**a**) Variation of the emission maxima with the bulk molar fraction of tetrahyrofuran (X_{THF}) and (**b**) the dependence of the local molar fraction (X_{THF}^{L}) on the bulk molar fraction of tetrahydrofuran (X_{THF}) in the mixture of cyclohexane and tetrahydrofuran. The solid lines represent the properties of an ideal mixture. The dashed lines stand for the fitted curves using eq. 7 for (**a**) and eq. 6 for (**b**). The fitted parameter for $\overline{\nu}_{em,max12}$, $f_{2/1}$ and $f_{12/1}$ are 22076 cm^{-1}, 32.3 and 29.8, respectively.

23

Figure 8.
Time-resolved and steady-state fluorescence spectra of 1-amino-5-isocyanonaphthalene (ICAN) in acetonitrile. Curves with symbols represent the time-resolved spectra recorded at $\Delta t = 2.6$ ns intervals. The solid grey curve represents the steady-state fluorescence spectrum.

Figure 9.
Variation of the fluorescence emission intensity (**a**) and maximum (**b**) of ICAN in water in the presence of sodium laurylsulfate (SLS) with the logarithm of SLS concentration. Experimental conditions: Concentration of ICAN = 4.7×10^{-6} mol/L, $\lambda_{ex} = 336$ nm, T=25 ^{o}C.

24

Scheme 1.
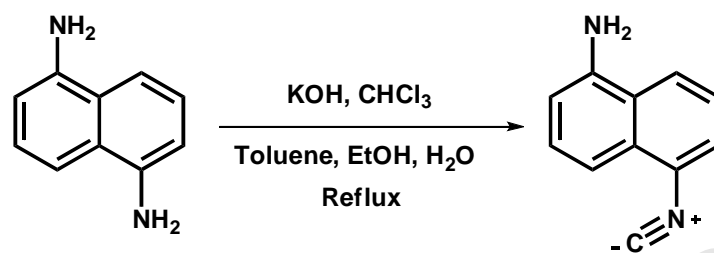
Figure 1.

Figure 2.

Figure 3.

28

Figure 4.

Figure 5.

30

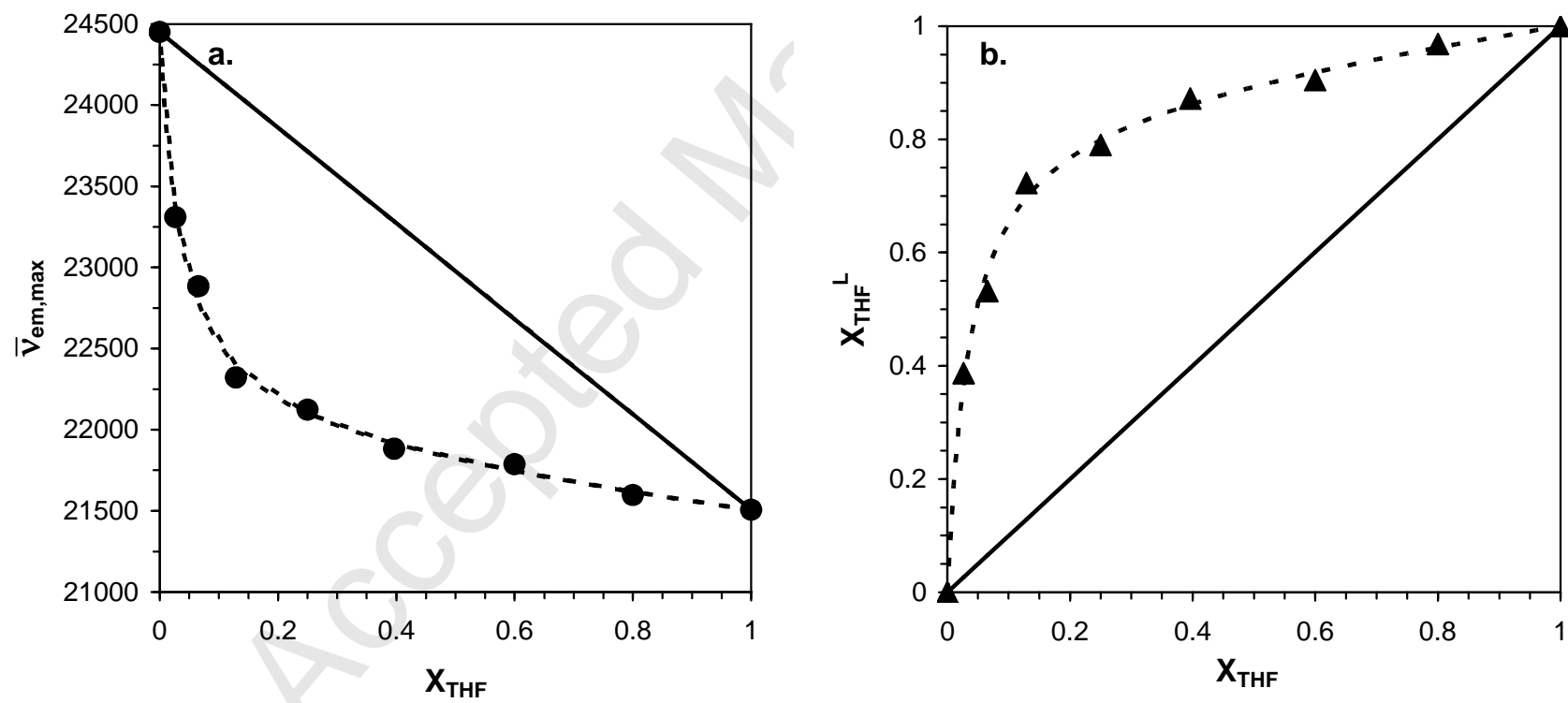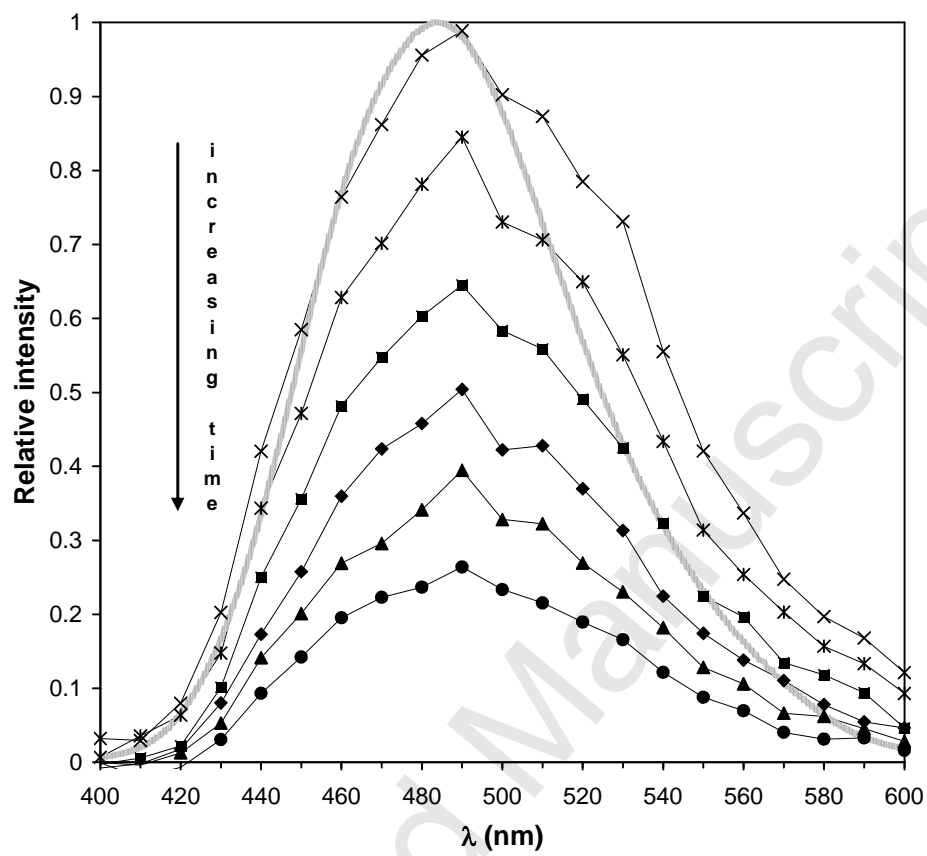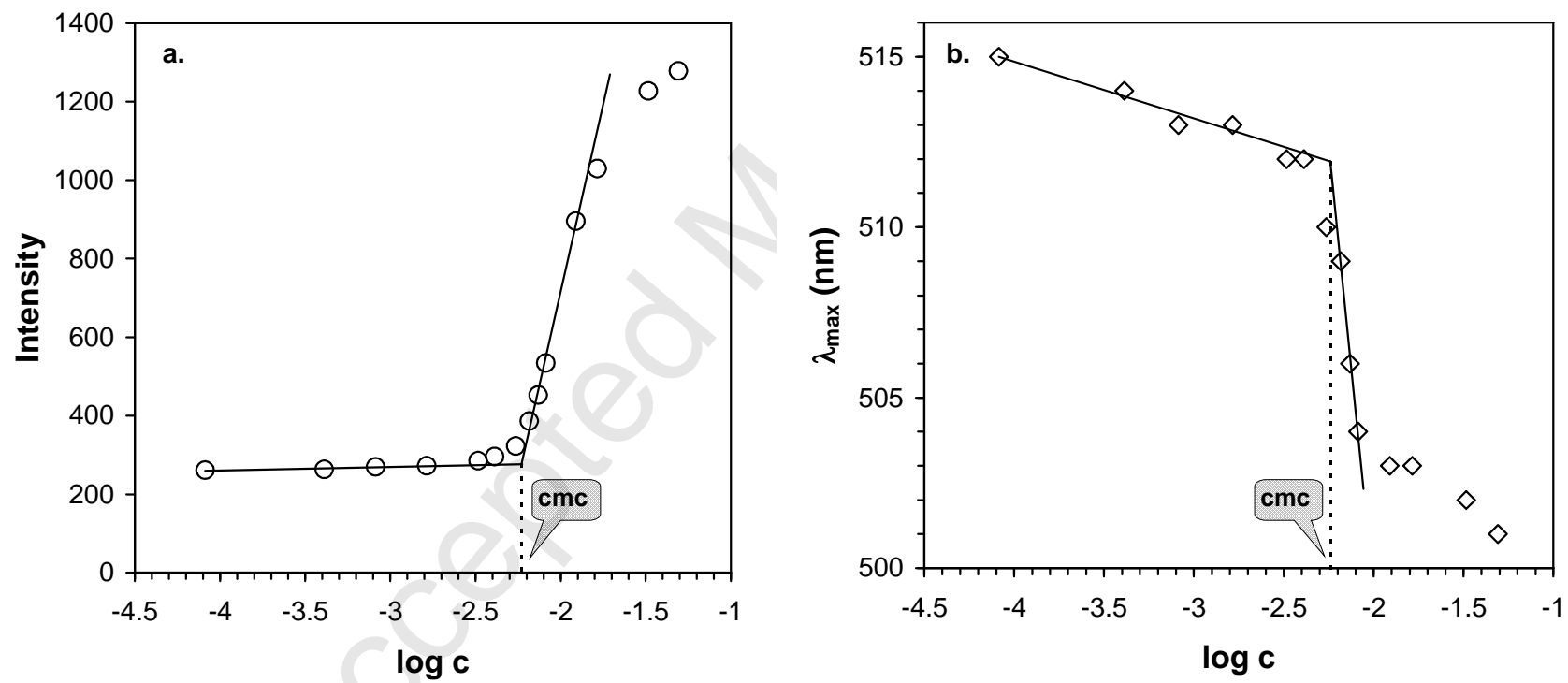**Figure 6.**

31
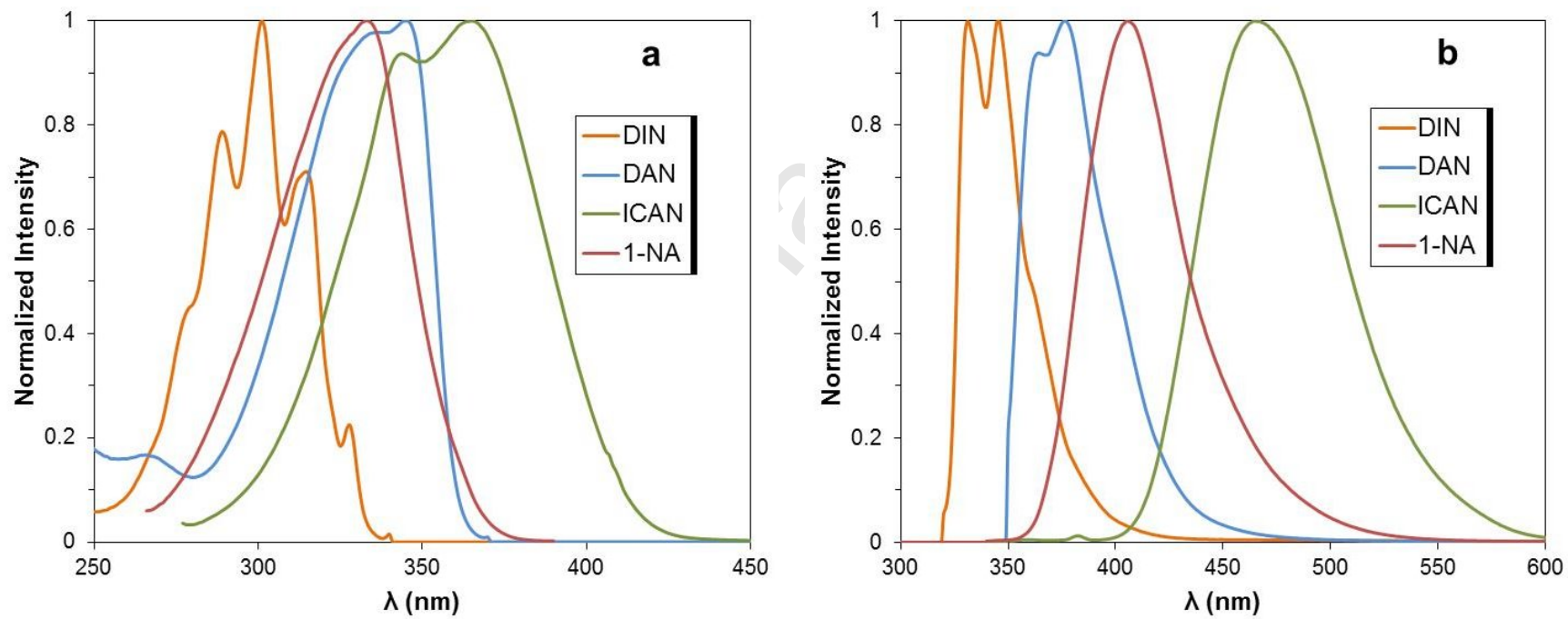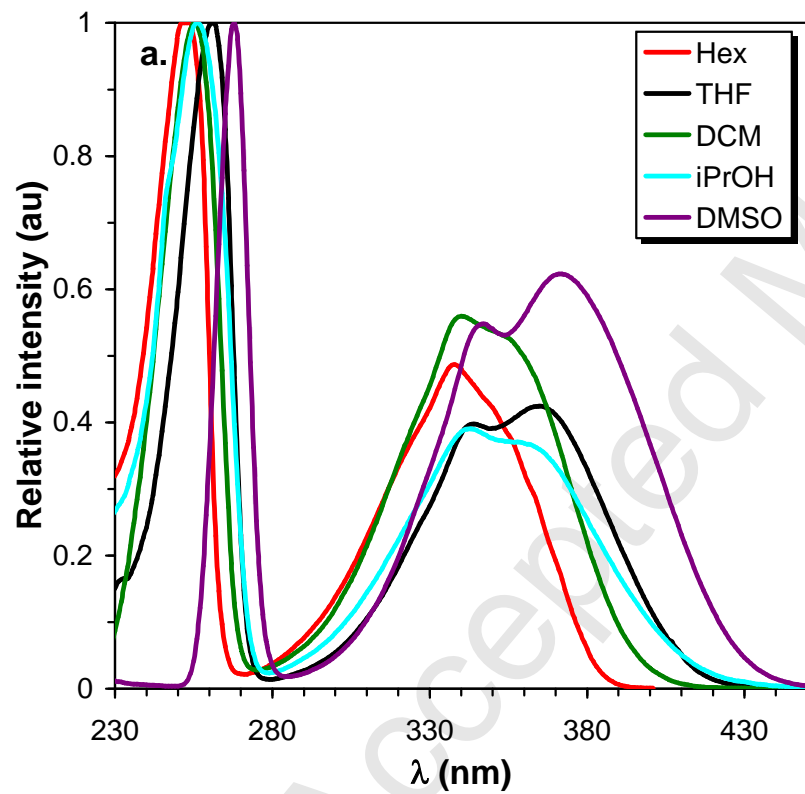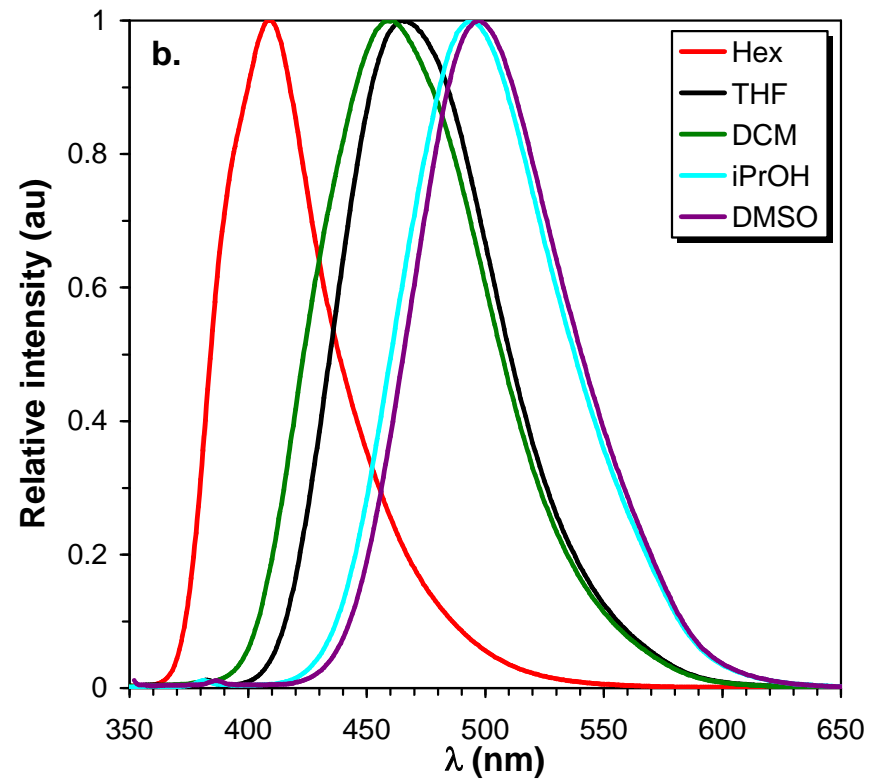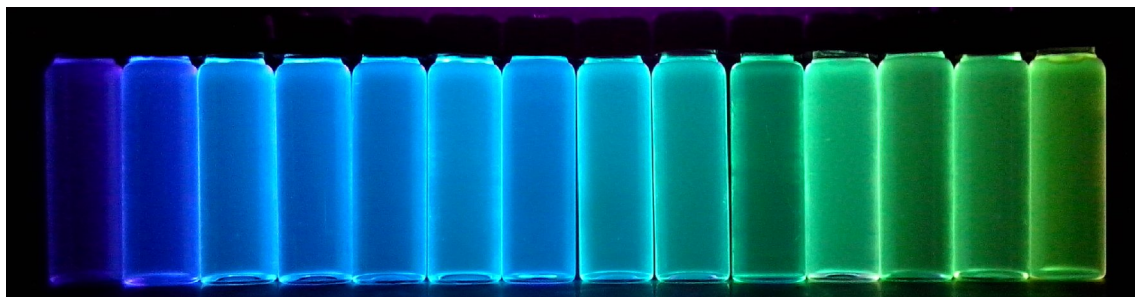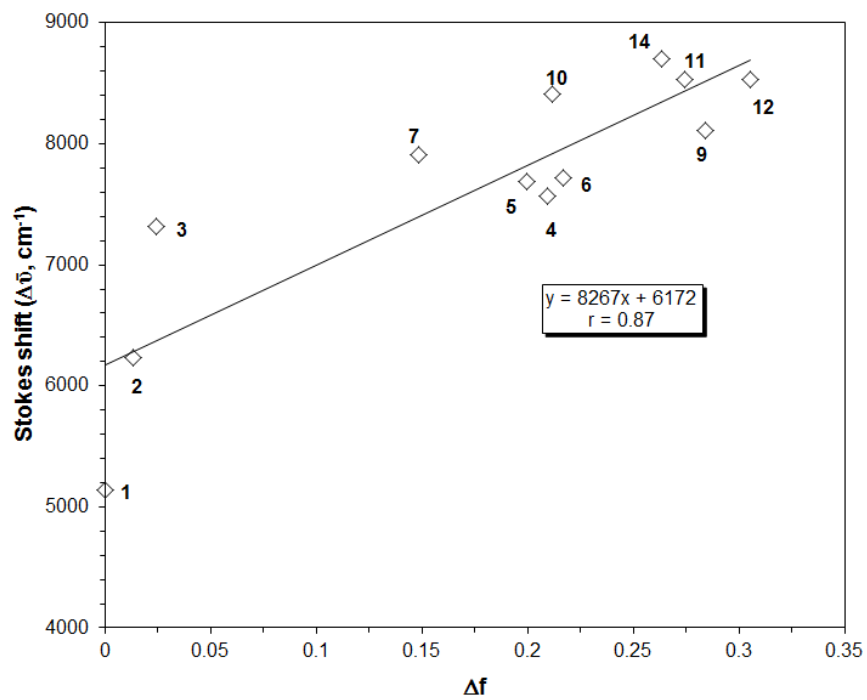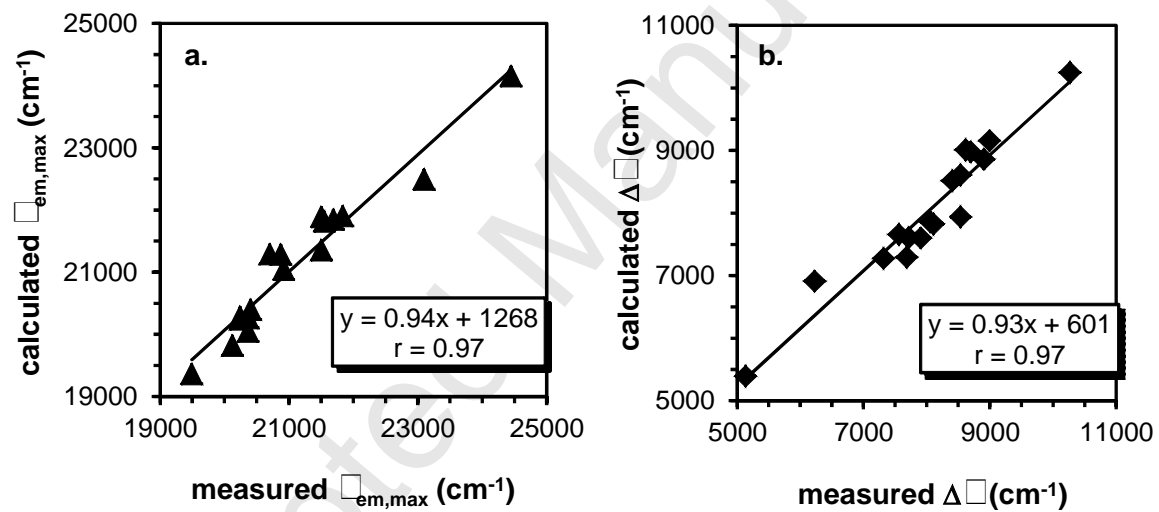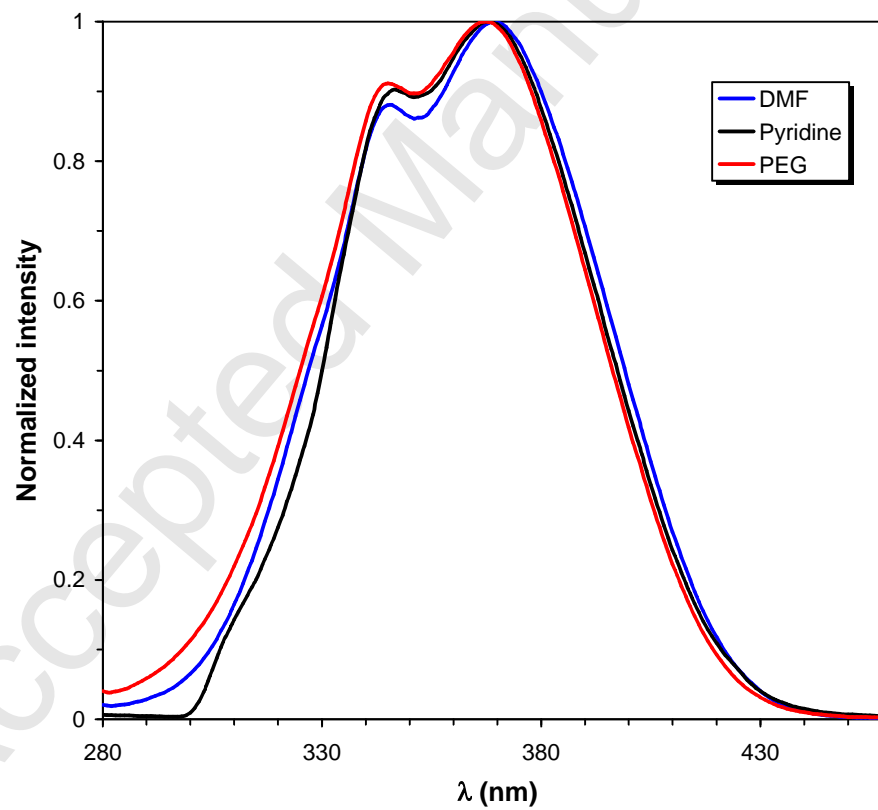
Figure 7.

**Figure 8.**

Figure 9.

Highlights

A new isocyanide containing naphthalene based fluorophore was prepared.

The molecule showed positive solvatochromic effects.

The optical properties were studied by steady-state and time dependent fluorescence spectroscopy.

Lippert-Mataga and Kamlet-Taft equations were used to describe the solvatochromic properties.

The molecule showed preferential solvatation in THF and can be used for cmc determination.

35
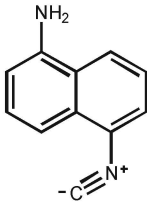
Positive Solvatochromism

$\lambda_{em,max}$ = 409-513 nm

ϕ_f = 0.04-0.95